ABSTRACT

MODELING OF QUAD-STATION MODULE CLUSTER TOOLS USING PETRI NETS

by
Aung Nay

The semiconductor industry is highly competitive, and with the recent chip shortage, the throughput of wafers has become more important than ever. One of the tools that the industry has deployed is to use of quad-station modules instead of the traditional single-station modules that allow for higher throughput and better wafer consistency by processing multiple wafers at the same time and distributing work. The industry trend is to use multiple transfer chamber robots to stack the quad-station modules in a series, particularly for etch products. In this work, the quad-station cluster tool wafer movement is modeled by using Petri net as a process-bounded system. The system analysis and simulations are performed by using timed and colored Petri nets. The results are useful to deepen our understanding of the discrete-event dynamics of quad-station module cluster tools and offer the highly needed insight into their efficient and deadlock-free operation.

MODELING OF QUAD-STATION MODULE CLUSTER TOOLS USING PETRI NETS

by
Aung Nay

A Thesis
Submitted to the Faculty of
New Jersey Institute of Technology
in Partial Fulfillment of the Requirements for the Degree of
Master in Computer Engineering

Department of Electrical and Computer Engineering

December 2022

APPROVAL PAGE

MODELING OF QUAD-STATION MODULE CLUSTER TOOLS USING PETRI NETS

Aung Nay

Dr. Mengchu Zhou, Dissertation Advisor — Date
Distinguished Professor of Electrical and Computer Engineering, NJIT

Dr. Tao Han, Committee Member — Date
Associate Professor of Electrical and Computer Engineering, NJIT

Dr. Xiwang Guo, Committee Member — Date
Associate Professor of Computer and Communication Engineering College, Liaoning Petrochemical University, Fushun, 113001, P R. China

BIOGRAPHICAL SKETCH

Author:	Aung Nay
Degree:	Master
Date:	December 2022
Date of Birth:	
Place of Birth:	

Undergraduate and Graduate Education:

- Master of Science in Computer Engineering,
  New Jersey Institute of Technology, Newark, NJ, 2022

- Bachelor of Arts in Economics,
  The Ohio State University, Columbus, OH, 2007

Major:	Computer Engineering

To my partner in good and bad, ✊!

ACKNOWLEDGMENT

This work would not have been possible without Prof. Mengchu Zhou's inspiration, direction, and guidance. I am very much in debt to Prof. Zhou for his generosity, for the opportunities he has freely shared, and for being a great teacher who hooked me into the subject matter more than any other teacher I have ever had.

I am also very thankful to Dr. Side Zhao for giving me a glimpse into the semiconductor industry with a warm welcome and opening the door to a wonderful world full of good human beings.

I would also like to thank the committee members: Prof. Xiwang Guo and Prof. Tao Han, for being so generous and helping with the process.

I am very grateful to all my friends who worked with me along this learning journey: Megha, Salman, Aftab, Cynthia, Ravi, and Brendan.

I want to thank my mom and dad for giving me opportunities to build foundational knowledge and developing my ability to persevere.

Most importantly, I thank the most important individual in my life, my wife, Aye. She has been a constant source of support, encouragement, and joy through challenges. She inspires me to aspire to be a little better every day. I cannot imagine my life without Aye.

TABLE OF CONTENTS

TABLE OF CONTENTS
(Continued)

LIST OF TABLES

LIST OF FIGURES

LIST OF VIDEOS

CHAPTER 1

INTRODUCTION

The semiconductor industry is highly competitive, and with the recent chip shortage, the throughput of wafers has become more important than ever. One of the tools that the industry has widely deployed is to use quad-station modules instead of the traditional single-station modules that allow for higher throughput and better wafer consistency by processing multiple wafers simultaneously. The industry trend is to use multiple transfer chamber robots to stack the quad-station modules in a series, particularly for etch products. In this work, the quad-station cluster tool wafer movement is modeled by using Petri nets. As a process-bounded system, such a cluster tool is described via timed and colored Petri nets. Its detailed analysis and simulations are conducted in this thesis work.

1.1 Overview

This thesis work models a production semiconductor quad-station process module cluster tool by using Petri net. The model is then analyzed for reachability, boundedness, liveness, and reversibility by using TINA and simulated for wafer movements by using CPN Tools. This is an exploration to see if Petri net scheduling can be pragmatically implemented in a production environment. Currently, the industry uses a heuristic rule-based approach to schedule cluster tools as it is flexible, extensible, and provides near or quasi-optimal solutions. However, it relies on a developer's experience and creativity. Any mature ruleset for a new tool configuration is derived through trials and errors and, as such, compromises the quality and reliability of the scheduler component in its initial stage. As tool complexity increases, the complexity of the scheduler component becomes higher and higher. Using the Petri Nets is not an outright rejection of a heuristic approach. In fact, Petri Nets can be used in conjunction with various heuristic approaches, according to [6] [14].

1.2 Cluster Tool Background

Cluster tools process wafers for the fabrication of micro-electric components using automated robotic manufacturing systems. [9] [10] [15] [19] [20] Cluster tools are systems that allow for the transfer of wafers process modules (PMs), buffers, and loadlocks. They can be used for the parallel process of multiple wafers for improved throughput. The general configuration of a cluster tool includes multiple PMs, one or more transfer chambers, and loadlocks. Beyond the loadlocks, the system is operated under a vacuum environment using one or more robotic arm(s) to prevent contamination or other undesired reactions.

Until recently, due to limited floor space in fabs, cluster tools tend to have no more than six process modules, which tend to be single-station process modules. However, with the need for higher productivity and throughput, quad-station process modules are being introduced with some cluster tools supporting up to ten process modules.

In a typical operation, unprocessed wafers are transferred to the cluster tools in FOUPs (Front Opening Unified Pods). FOUPs generally hold 25 wafers. Most cluster tools have the capacity to handle multiple FOUPs. Upon the arrival of FOUP to a cluster tool, the unprocessed wafers are transferred by the atmosphere robotic arm(s) into the loadlock, which are airlocks that reduce the pressure to vacuum for the transfer chamber and PM operations. In some systems, aligners are used to align the wafers to the proper orientation for processing purposes.

Once the wafers are in the transfer chamber, they are quickly moved to the appropriate PM for the recipe that is being used. Some recipes call for PM revisits, meaning that the wafer will visit a specific PM more than once. Once processing is complete, the wafers are removed from the system through the loadlocks back to the FOUPs. In some processes, there are time constraints on how long a wafer can remain in the PM, and there are also some requirements for stay uniformity for quality control purposes.

Depending on the process, PMs generally need to be cleaned after each operation, with non-zero cleaning time. Quad-station modules have an advantage here as the PM only needs to be clean after processing four wafers instead of one. Quad stations also break down the operation into four sub-operations, improving the uniformity of wafers.

In the process, the graph aspect of the reachability graph is also explored and can be found in the Appendix. The rest of the document is organized as follows. Chapter 2 describes cluster tools in general and introduces why quad-station modules are being used. Chapter 3 goes over the basic definitions of Petri nets. Chapter 4 is the description of the cluster tool being modeled. Chapter 5 is the Petri net model of the cluster tool. Chapter 6 is the simulation and analysis of the Petri net model. And chapter 7 concludes the thesis.

CHAPTER 2

PETRI NET OVERVIEW

Petri nets are one of the modeling tools available to simulate, evaluate, and model different mechanisms, operations, and procedures [7] [8]. Petri Nets bring the mathematical and graphical aspects of modeling different scheduling problems in event-driven systems.

2.1 Petri Net Basics

It supports the representation of asynchronous, sequential, and concurrent operations through the structure and dynamics of discrete event systems. [5] We can model the flow of information and controls in systems using Petri nets. And most importantly, we can use the analytical properties of Petri net, such as reachability, boundedness/safeness, lightness, and reversibility, to understand the problems better. [5] Petri nets are directed bipartite graphs with places and transitions with static (inputs and outputs) and dynamic (executions and events) properties. There are many variants of the "basic" Petri nets, which include extensions and abbreviations. Some variants of notes include edge types, which allow for extended control of the systems; time, which allows for performance analysis; color, which allows for model attributes; and hierarchy, which allows for the structuring of models. [13]

As we can see in Figure 2.1, the concept of Petri net is easy to follow. Let's say you have the following items: 4 cups of water, 3 cups of sugar, and 2 cups of lime juice. We want to make lemonade and then serve the lemonade in glasses (not equivalent to a cup) that you recently bought. According to a simple google search, the lemonade recipe calls for 3 cups of water, 1 cup of sugar, and 1 cup of lime juice. Once you make lemonade, you will get a total of 6 glasses of lemonade. All this information can be seen in State 0 of Figure 2.1. The tokens (dots) that are in the input places (circles) to the transition (rectangle) tell us how many resources we have. Based on the arc weights, we can evaluate if we can even attempt to make lemonade (this is called whether the transition can be enabled or not). We can say the transition is enabled if we have enough resources to make lemonade. That does not mean we will make lemonade. It just means that we have the resources to make lemonade. If we did make lemonade (that is firing the transition), we would get six glasses of lemonade. State 0 is the state prior to firing the transition, meaning the event of making lemonade, and State 1 is the state after firing the transition. In State 1, we can see that we have used up 3 cups of water, a cup of sugar, and lime juice each. We now also have six glasses of lemonade.

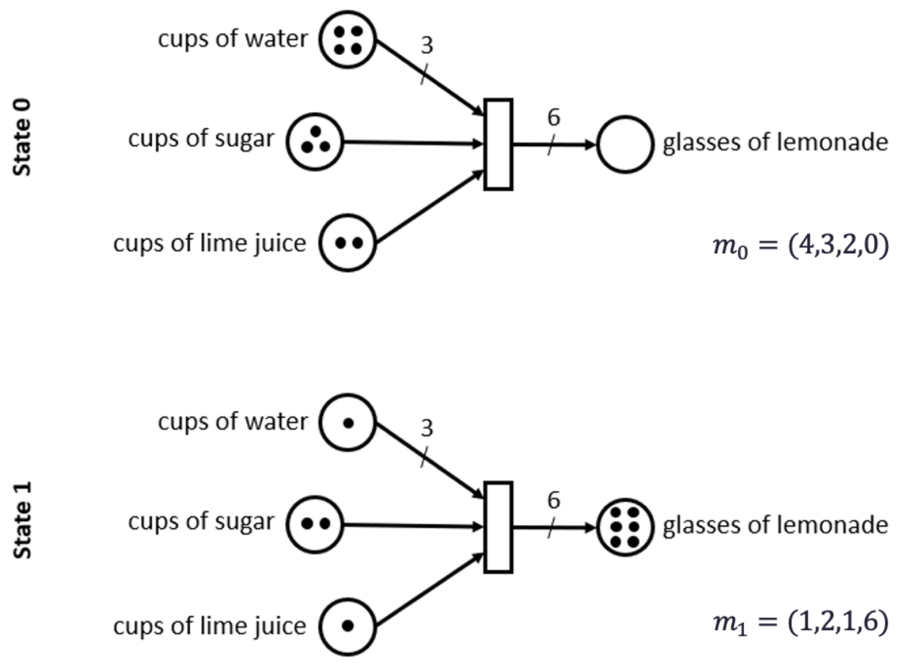

Figure 2.1 Petri net example with two states on making lemonade.

2.2 A Marked Petri Net Formal Definition

The general marked Petri Net [11] [17] [21] can be described formally as follows. A marked Petri net $(PN)\ Z = (P, T, I, O, m)$ is a five-tuple where:

- $P = \{p_1, p_2, \ldots, p_n\}$. $n > 0$, is a finite set of places pictured by circles;
- $T = \{t_1, t_2, \ldots, t_n\}$. $n > 0$, is a finite set of places pictured by bars, with $P \cup T \neq \emptyset$ and $P \cap T \neq \emptyset$;
- $I: P \times T \rightarrow N$, is an input function that defines the set of directed arcs from P to T where $N = \{0,1,2,\ldots\}$;
- $O: P \times T \rightarrow N$, is an output function that defines the set of directed arcs from T to P;
- $m: P \rightarrow N$, is a marking whose i th component represents the number of tokens in the i th place. An initial marking is denoted by m_0. Tokens are represented by dots.

The four-tuple (P, T, I, O) is called a Petri Net structure that defines a directed graph structure.

Enabling: t is enabled at marking m

- if $\forall\, p \in P, m(p) \geq I(p, t)$.

Note: If $I(p, t) = 0$, the above equation holds regardless of $m(p)$. If t has k input places, k such relations must hold simultaneously.

Enabling means that if a place belongs to the Petri net in question, there need to be enough tokens in the place that is required by the transition's input. For example, if the transition input requires two tokens, the place needs to have at least two tokens to enable the transition. The most important thing to note here is that just because a transition is enabled does not mean it would necessarily fire. It just has the potential to fire.

Firing: An enabled transition t at m can fire, yielding a new marking m' such that

- $\forall\, p \in P, m'(p) = m(p) - I(p, t) + O(p, t)$

This is applicable to all Petri nets.

The firing means that when an enabled transition fires, it will create a new state (m'). The change between the old state (m) and the new state (m') is for each of the places that are related to this particular transition, one must take away the tokens that are required for firing the transition and add the tokens that are the result of the firing of the transition. This means that when a transition has been enabled, the transition can fire.

2.3 Anti-Place Definition

The definition of an anti-place [2] is such that it has a corresponding original place with two transitions that are inputs and outputs for the place. As shown in Figure 2.2, we have p_0, place, and the anti p_0, anti-place. The transition t_0 has outputs going into p_0, and the transition t_i has inputs from p_0 in Petri net without anti-place. To create an anti-place and impose a capacity limit on p_0, we must first create an anti-place, anti p_0, then connect arcs from anti p_0 to t_0 and from p_i to anti p_0. The key thing here is that the weight of the arc goes from anti p_0 to t_0 must match the arch going from t_0 to p_0, and the arc goes from t_0 to anti p_0 must match the arch going from p_0 to t_i. They are accounting for the tokens going in and out of p_0. Then, we must place tokens in anti p_0 such that $M(anti\, p_0) = K(p_0) - M(p_0)$, meaning the finite capacity we are imposing on p_0 is equal to the total number of tokens in p_0 and anti p_0. (If we have colored tokens going from t_0 to p_0 and to t_i, we must make sure that the tokens go from and to anti p_0 are either uncolored or of a different color.) By adhering to the total number of tokens, there can only be a maximum of $K(p_0)$ tokens at p_0. We can use this approach to limit the capacity of not just a single place but also multiple places that are capped by a pair of transitions.

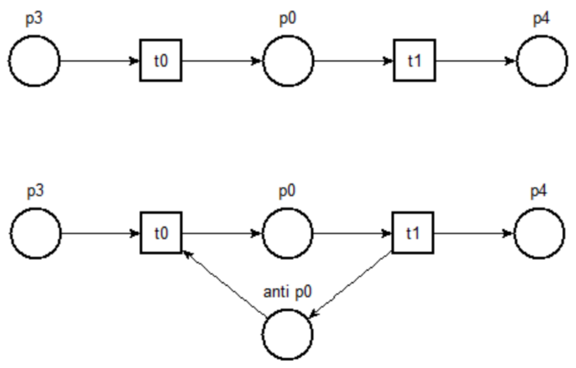

Figure 2.2 Anti-place example.

CHAPTER 3

CLUSTER TOOL OVERVIEW

The cluster tool being modeled is a semiconductor production unit used for 3D NAND production by various storage manufacturers.

3.1 Description of Cluster Tool

As shown in Figure 3.1, it has four quad-station process modules, two transfer chambers with dual arms with a single hinge in each, a buffer with five slots for wafers, an atmosphere arm that operates between carrier handlers and the airlocks, and an aligner. In this study, we assume that the scheduling time is process-bound, the wafers have a single recipe, and all PMs run the same recipe. The raw wafers from the carrier handlers are picked up by the atmosphere arm and are aligned prior to being inserted into the loadlocks. Once the wafers enter the vacuum chamber, they visit a single PM. Depending on the PM being visited, the path taken by the wafer differs in the initial and final transient processes. However, during the steady-state, all wafers travel the same path through the vacuum buffer; that is, the wafer travels as follows: Carrier Handler -> Aligner -> Loadlock -> Vacuum Buffer -> PM -> Vacuum Buffer -> Loadlock -> Carrier Handler. The single-arm robot handles the transfer operation between the carrier handler and the loadlock, including the aligner. As for the transfer operation between the loadlock, PMs, and the vacuum buffer, they are handled by the dual-arm robots in transfer chambers 1 and 2. Transfer chamber 2 is responsible for transfer operations between the vacuum buffer and either PM_2 or PM_4, while transfer chamber 1 is utilized for transfer operations between the loadlocks, vacuum buffer, and either PM_1 or PM_5. All the PMs are quad-station modules (QSM), and the vacuum buffer has a capacity for five wafers. The aligner can align only one wafer at a time.

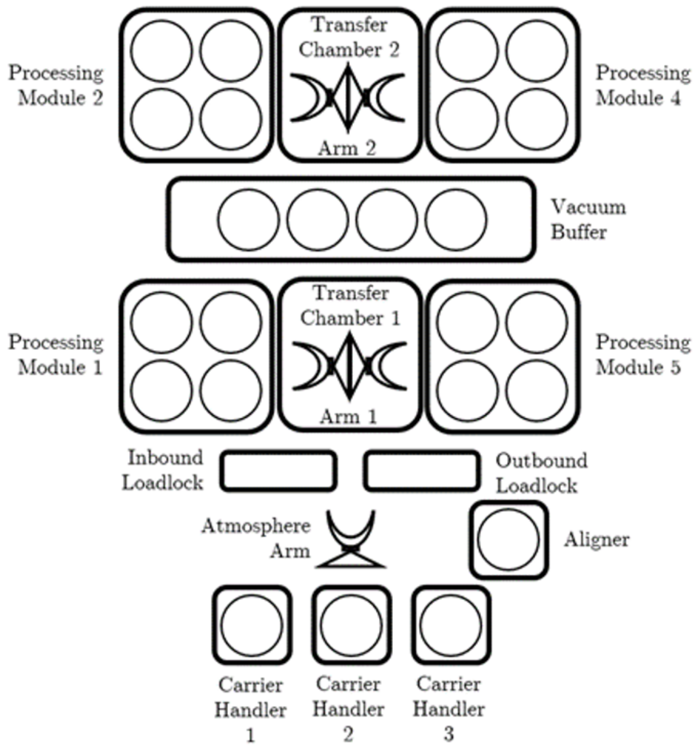

Figure 3.1 Quad-station cluster tool for modeling.

CHAPTER 4

PETRI NET MODELS OF CLUSTER TOOLS

In this section, we model the cluster tool described in Chapter 3, which is a cluster tool with quad-station processing modules.

4.1 Modeling Resource-Oriented Model

Modeling using Resource-Oriented Petri net [13] is split into three categories:

1. steady-state
2. initial transient process (batch begin)
3. final transient process (batch end).

For this particular model, the process is neither multi-visit nor repeating, meaning the wafer only has to visit one PM and exits after the process. Hence, the Petri net combines four resource-oriented Petri nets for each PMs with a cyclic process. The four Petri nets, when combined, share resources, including the robotic arms, vacuum buffer, loadlocks, and atmosphere components. (Please see below for "Notations.") In this single PM steady-state Petri net, as you can see in Figure 4.1, at PM_i, there is a swap operation [5] of wafers between PM_i and the vacuum buffer whereby an unprocessed wafer is picked up from the vacuum buffer, then a processed wafer is removed from the PM_i, and an unprocessed wafer is inserted into the PM_i, after which the processed wafer is placed into the vacuum buffer. There are two different operations with the loadlock: a swap operation and a single wafer operation. During the swap operation, a processed wafer is placed into the outbound loadlock, and an unprocessed wafer is picked up from the inbound loadlock. There is also an independent process of transferring processed wafers to the outbound loadlock and unprocessed wafers from the inbound loadlock. In addition, the atmosphere arm handles the transfer of wafers between the loadlocks, aligner, and the FOUP. This description is for the standard recipe process in which a single wafer is moved into the PM at a time, and the individual wafer(s) are processed separately.

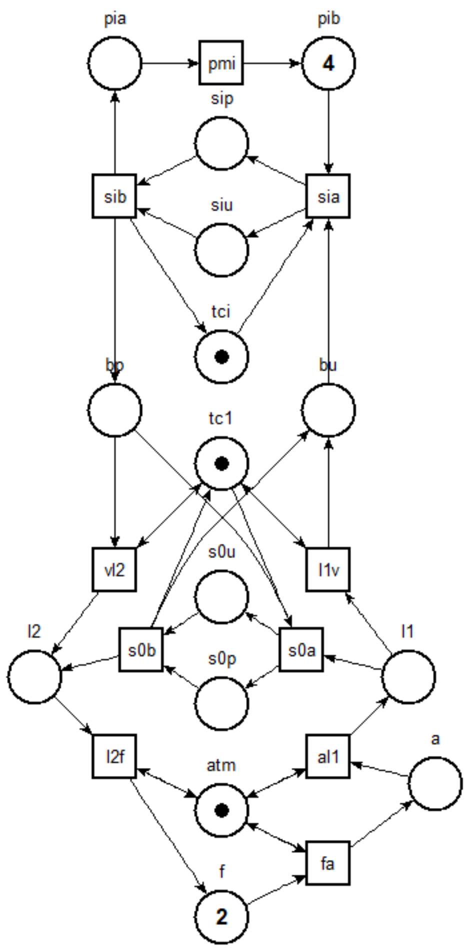

Figure 4.1 Steady-state Petri net for a single process module.

In contrast, Figure 4.2 describe the model in which we can use the static recipe process that processes four wafers at a time. One thing we should note here is that we are only using one token for the robot arms (tc_1 and tc_i), which generally is associated with single-arm robots. However, in our case, the dual-arm robots are used in single operations to either swap or simple transfers. Hence, the use of a single token for the robot arms. In this Petri net model, the weight of the arcs for the transfer operation with PM_i is 1, meaning we are just modeling for a single robot with dual arms with dedicated arms for processed and unprocessed wafers. To change this into a single robot with quad arms with dual processed and unprocessed arms, we can simply change the transfer operation arc weights and swap place capacity to 2. For such a change, we can also assume that the aligner can align two wafers simultaneously for model simplification.

Note: All Petri net analyses are done in TINA (Time petri Net Analyzer), and visual simulations are done in CPN Tools.

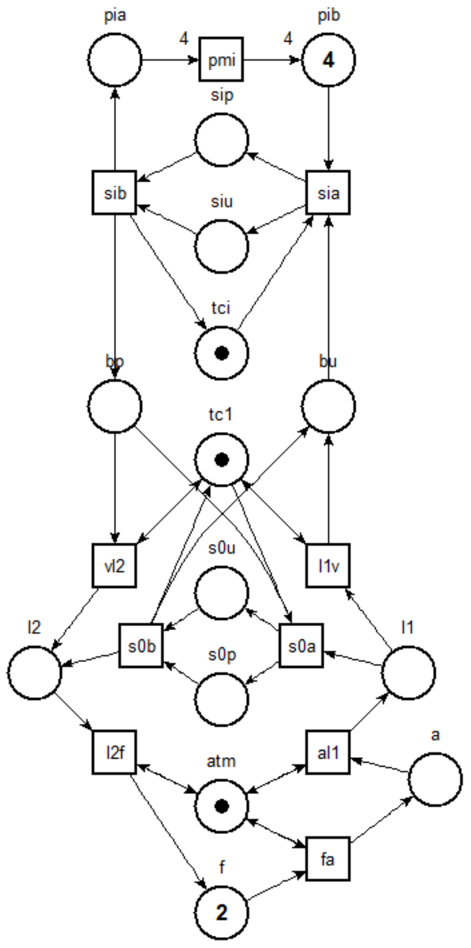

Figure 4.2 Steady-state Petri net for a single process module using a static recipe.

4.2 Finite-Capacity Petri Net

A finite capacity Petri net $(PN)Z = (P, T, I, O, m, K)$ is a six tuple where, in addition to the same five definitions of the tuples as above:

$K: P \rightarrow N - \{0\}$ is a capacity function where $K(p)$ represents the maximal number of tokens that p can hold

Enabling of a finite capacity Petri net: t is enabled at marking m:

- If $\forall p \in P$, the following two conditions must hold true:
    - $m(p) \geq I(p,t)$ and
    - $K(p) \geq M(p) - I(p,t) + O(p,t)$

The firing definition remains the same as the prior definition above.

The main difference between a finite capacity Petri net and a Marked Petri net is that places that have a finite limit have a capacity limit for the places, meaning if the change in the number of tokens, by firing a transition, exceeds the limit of the place, the transition would not be enabled to begin with.

4.3 Notations

Below are the notations used for the model, including its places, transitions, and anti-places, as well as their conditions, capacities, and some definitions. The last sub-section also includes the table for the time durations of activities and operations.

Let $\mathbb{N}_n = \{1,2,4,5\}$ and $\Omega_{n\_}n = \mathbb{N}_n \cup \{0\}$.

4.3.1 Places

Places are represented by circles. They model resources, buffers, conditions, or states.

- f: FOUP/Carrier Handler
- a: Aligner with $K(a) = 1$
- atm: Atmosphere Arm
- l_1: InboundLoadlock $K(l_1) = 1$
- l_2: Outbound Loadlock $K(l_2) = 1$
- tc_1: Transfer Chamber 1 (with dual-arm robot) with $K(tc_1) = 1$
- tc_2: Transfer Chamber 2 (with dual-arm robot) with $K(tc_1) = 1$
- b_u and b_p: These are virtual vacuum buffers for unprocessed and processed wafers, respectively, where $K(b_u) + K(b_p) = 5$. They are, in fact, a single unit with five wafer capacities.
- p_{ia} models the pre-processing condition at $pm_i, i \in \mathbb{N}_n$, where $\mathbb{N}_n = \{1,2,4,5\}$ with $K(p_{ia}) = 4$
- p_{ib}models the condition post-processing conditions at $pm_i, i \in \mathbb{N}_n$, where $\mathbb{N}_n = \{1,2,4,5\}$ with $K(p_{ib}) = 4$
- s_{iu} models the movement of the unprocessed wafer during the swap operation, as well as the wait time, at $pm\_i, i \in \Omega\_n$, where $\mathbb{N}_n = \{0,1,2,4,5\}$ with $K(s_{iu}) = 1$
- s_{ip} models the movement of the processed wafer during the swap operation, as well as the wait time, at $pm\_i, i \in \Omega\_n$, where $\mathbb{N}_n = \{0,1,2,4,5\}$ with $K(s_{ip}) = 1$

4.3.2 Transitions

Transitions are represented by rectangles. They model events, transformations, or transportations.

- s_{i1} models the beginning of the swap process between a processed and unprocessed wafer at $pm_i, i \in \Omega\_n$, where $\mathbb{N}_n = \{0,1,2,4,5\}$
- s_{ib}models end of the swap process between a processed and unprocessed wafer at $pm_i, i \in \Omega\_n$, where $\mathbb{N}_n = \{0,1,2,4,5\}$
- pm_i models the processing of wafers at $pm_i, i \in \Omega\_n$, where$\mathbb{N}_n = \{1,2,4,5\}$

- l_1v and vl_2: models the movement of a wafer from loadlock to the vacuum buffer and vice versa
- al_1: models the movement of a wafer from the aligner to the loadlock
- fa: models the movement of a wafer from the FOUP to the aligner
- l_2f: models the movement of a wafer from the loadlock to the FOUP

4.3.3 Anti-Places

Anti-Places are capacity control for corresponding places. The anti-places are not shown in the Petri net model images. But only in the simulation videos, as the CPN Tools does not support finite capacity Petri nets.

- ta: anti-place for aligner
- tl_1: anti-place for loadlock 1
- tl_2: anti-place for loadlock 2
- tb: anti-place for the combined places of b_u, buffer for unprocessed wafers, and b_p, buffer for processed wafers

4.3.4 Time Durations

The time durations for different activities in the cluster tools are defined as follows in table 4.1. It includes different robot activity times and the corresponding wait times, as well as other components and their processing time and their wait times.

Table 4.1 Time Durations For Different Activities In The Cluster Tool

Symbol	Transition or Place	Action	Duration allowed
μ		Any robot arm movement	
σ	s_{ia}, s_{ib}	Simple swap operation at PMi	
ω_{is}	s_{iu}, s_{ip}	Robot wait time at swap operation at PMi	$[0, \gamma]$
ω_{ip}	p_{ia}	Robot wait time at the beginning of swap operation at PMi	$[0, \infty]$
ω_{iz}	p_{ib}	Robot wait time at the end of the swap operation	$[0, \infty]$
ω_{il}	l_1v, vl_2, al_1, l_2f	Robot wait time at loadlock	$[0, \infty]$
ω_{ia}	al_1, fa	Robot wait time at aligner	$[0, \infty]$
ω_{if}	fa	Robot wait time at FOUP	$[0, \infty]$
τ_i	pm_i	Wafer being processed and waiting in PMi	$[a_i, a_i + \delta_i]$
λ	l_1, l_2	Loadlock time	
ρ	a	Aligner time	
ζ	pm_i	PMi processing completion time	
ζ_{ib}	pm_{ib}	Processing completion time at the first PM used in the initial transient process	
π		$(4\mu + \lambda + \omega_{il} + \rho + \omega_{ia} + \omega_{is} + \omega_{ip} + \omega_{iz})$ time for each wafer to get from FOUP to PMi	
ε	pm_i	PMi processing time	

CHAPTER 5

SIMULATION AND ANALYSIS

In this section, the Petri net model described in Chapter 4 is analyzed and simulated using TINA and CPN Tools, respectively.

5.1 Simulation and Analysis Overview

For analysis, TINA (Timed petri Net Analyzer) is used specifically to check for reachability, boundedness, liveness, and reversibility. The reachability graph of a Petri net provides a fundamental basis for the dynamic properties of a system. It allows us to determine whether our modeled system can attain a specific state due to a required functional behavior with a single or a sequence of events. It can also be used to check if there are any deadlocks in the system. In a bounded PN, the reachability problem is decidable, but the complexity is exponential. For boundedness, a Petri net is considered k-bounded or bounded if the number of tokens in each of the places is less than or equal to k, which is a finite value. The boundedness of the system allows us to determine if there are overflows in the system. A system's liveness tells us if there are any deadlocks in the system. If a system is not live, it means that there are deadlocks. However, there are different levels of liveness with regard to how many times a transition in a Petri net can fire, which ranges from 1 to k, where k $=$ every iteration. The reversibility of a PN tells us that the modeled system can go back to the original state of the system prior to firing of transition using a series of firings.

CPN Tools is one of the very useful tools to simulate Petri nets. CPN Tools can work with colored and timed Petri nets. It also uses a dialect of SML (Standard Markup

Language) to add additional functionality and control. However, it is no longer maintained, and some existing bugs hinder its use. Yet, for certain usages, omitting certain functionalities, it can still be a great tool. It is also the tool with the best documentation, although it can be outdated and irrelevant. The developers have moved on to Access/CPN tool, which is another Petri net tool based on CPN Tools but has significantly less functionality. CPN Tools was used as a visual simulator of wafer movement.

The wafers in the simulations are shown with changing green rectangles with rows of values. Each row has three distinct pieces of information:

- quantity of wafers of specific status and availability
- status of the wafer, whether it is unprocessed or processed (shown with either 'u' or 'p')
- time, in seconds, at which the wafer is available/ready

The format of the notation is as follows, split by ‘′’ and '@.'

```
Quantity'WaferStatus@Time
```

In some cases, the transition x_0 is used to simulate the cyclic nature of the system.

Each timed transition has a set constant delay specified by the prefix@+. There are additional places with finite tokens and arcs to model to finite capacity. There are also some inhibitor arcs that model a form of control.

5.2 Steady-State

The steady-state is defined as meeting the following conditions in the Petri net:

- $M(p_{ib}) = K(p_{ib}) = 4$, $i \in \mathbb{N}_n$, where $\mathbb{N}_n = \{1,2,4,5\}$
- $M(tc_i) \geq 1$, $i \in \mathbb{N}_t$, where $\mathbb{N}_t = \{1,2\}$
- $M(atm) = M(ta) = 1$

- $M(tl_i) = 1, i \in \mathbb{N}_t$, where $\mathbb{N}_t = \{1,2\}$
- $M(tb) = 5$

Each iteration of the steady-state starts at $\zeta_{ib} - \pi$. There is also an assumption that $\varepsilon \geq 16\pi$. The process of the steady-state as defined in the single PM, firing of $s_{ia}, i \in \mathbb{N}_n$, where $\mathbb{N}_n = \{1,2,4,5)$, transitions will depend on the availability of the processed wafers from each PM, which in turn is based on the optimized initial transient process, as the system is considered process bounded. This is straightforward for PM$_2$ and PM$_4$ as the arm is not shared with any other process. However, for PM$_1$ and PM$_5$, the arm is shared with the transfer operations in which wafers are moved from loadlocks to the vacuum buffer.

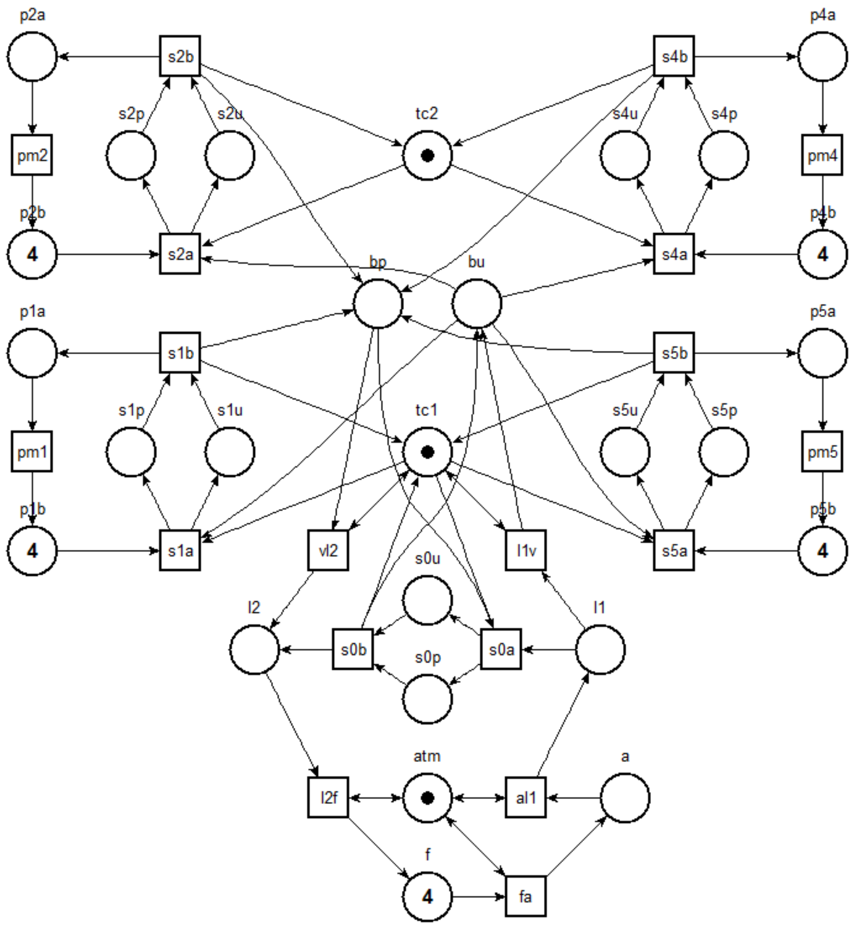

Figure 5.1 Steady-state Petri net.

As you can see in Figure 5.2, we can consider PM$_2$ and PM$_4$ as a sub-case, and is are much simpler to work with. Assuming a constant flow of unprocessed wafers into the vacuum buffer, as the wafer processing of each PM completes, the respective s_ia transition will fire and output wafers into the vacuum wafer, which is $K(b_p bp) + K(b_u) = 5$. We can even consider this as a system with two PMs without a buffer for simplicity. The availability of processed wafers will determine the order of the process, which is determined by the initial transient process. In Video 5.1, we see the simulation of the sub-net in which only PM$_2$ and PM$_4$ are considered, along with the buffers as the input and output of wafers.

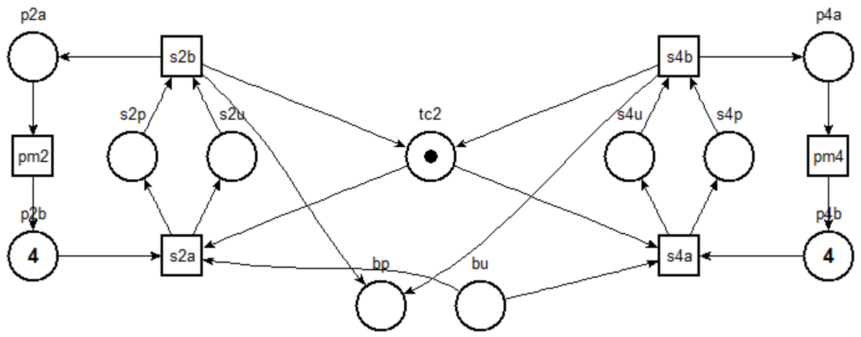

Figure 5.2 Steady-state Petri net only for PM$_2$ and PM$_4$.

There are delays associated with different transitions. Each swap transition has a delay of 8, and the PM transitions have a delay of 1800. The x_0 transition does not have any delays. The key thing to note in this simulation is the availability of wafers at PM$_4$. They are not available until time 200. This relative delay in the availability of the wafers at PM$_4$ and PM$_2$ allows us to operate this Petri net without any further controls. This setup consistently transfers four wafers to each PM, even though it is a standard recipe model. This would change once we simulate the whole system, and we will observe a behavior more consistent with the standard recipe, meaning the wafers will be inserted and processed one at a time across different PMs.

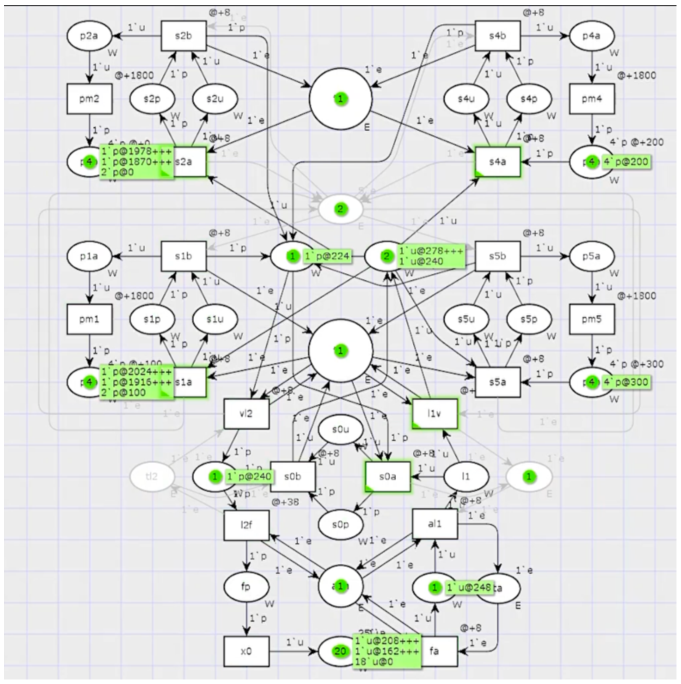

Video 5.1 Clip of video for steady-state simulation using CPN Tools available at https://www.youtube.com/watch?v=BX6NO9hwBk4.

We can also break down the steady-state Petri net into a subnet with only PM_1 and PM_5. If we look at Figure 5.3, we see that it behaves almost like a system with three PMs, where the buffer acts like a PM that does not require any processing, and wafers are immediately available. In addition, the input of wafers is available from two sources: PM_1 and PM_5 are fed by the buffers, while the buffer is fed by the loadlocks. In Video 5.3, we see a delay of 200 being deployed for PM_5, which allows us to have this PM without additional control. The swap at loadlock automatically happens whenever there is an unprocessed wafer in the inbound loadlock and a processed wafer in the vacuum buffer. Again, even though this is a standard recipe model, it consistently transfers four wafers to each PM and alternates between PM_1 and PM_5. When we combine everything and look at the whole system, the control mechanism required for it gets slightly different based on whether we would like to use a standard or static recipe.

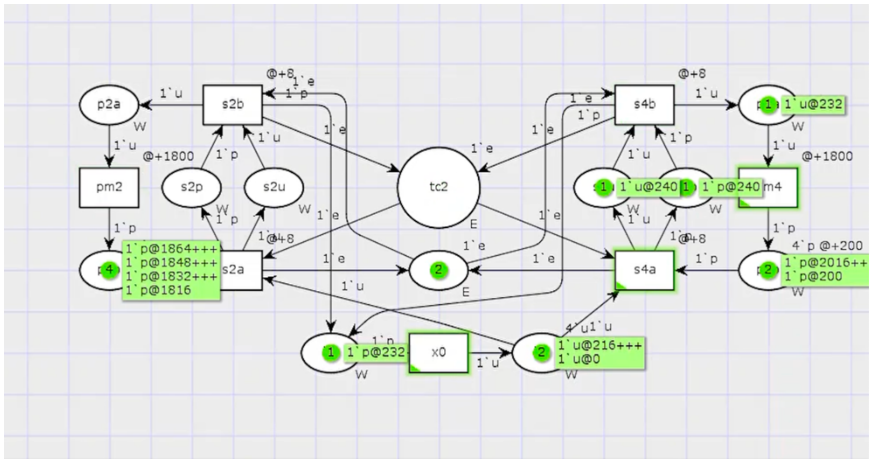

Video 5.2 Clip of video for steady-state simulation of only PM$_2$ and PM$_4$ using CPN Tools available at https://www.youtube.com/watch?v=ghXFskXlHFE.

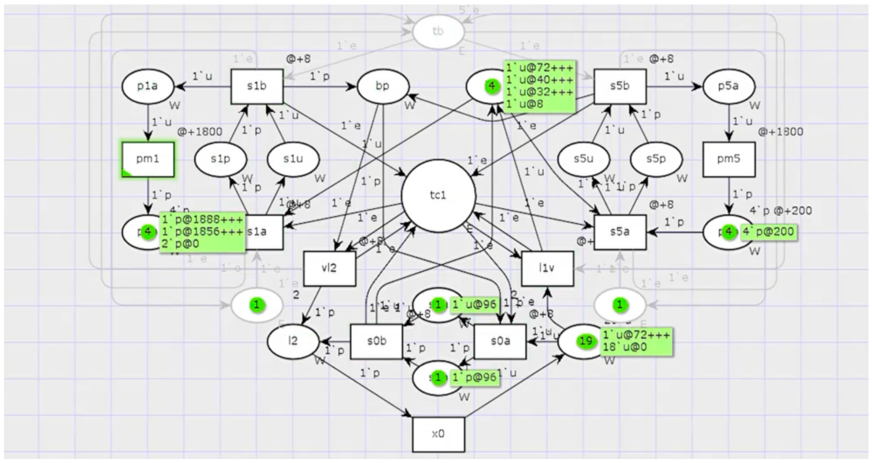

Video 5.3 Clip of video for steady-state simulation of only PM$_1$ and PM$_5$ using CPN Tools available at https://www.youtube.com/watch?v=IwZA9bdtHsI.

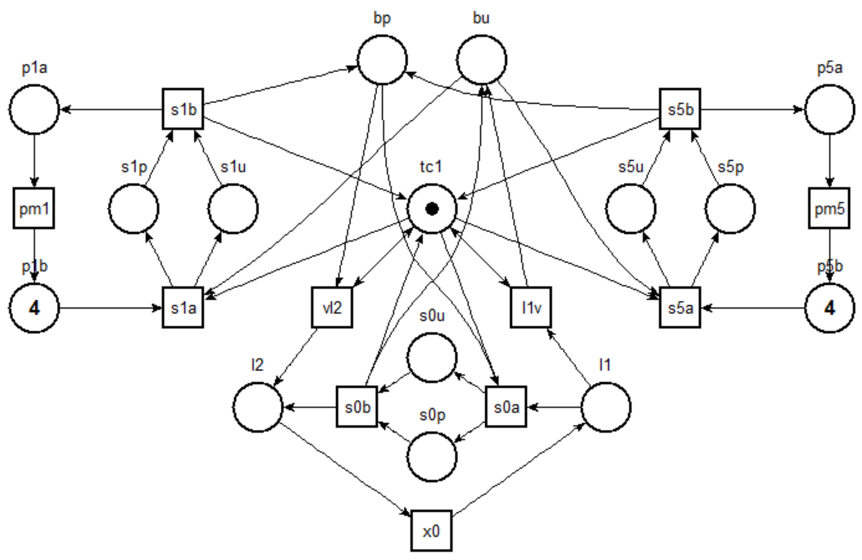

Figure 5.3 Steady-state Petri net only for PM_1 and PM_5.

When considering the standard recipe, the first approach of using delays for simulating the availability of the processed wafers from the PMs starts with processing each wafer. For example, all four wafers from PM_1, in Video 5.4, are available at time 100. However, as it is a free choice Petri net, the system will randomly pick any of the PMs with the available processed wafer to swap. When we look at the static recipe model, using delays for the availability of the wafers does not work as the Petri net behaves in a manner similar to the standard recipe and transfers individual wafers to different PMs based on their availability. However, this is addressed using the transition priority, as shown in Video 5.5. The s_{ia} transitions have different priorities, meaning since the system is process bounded, the priority transitions behave like a control system in which the wafer transfers are iterated through different PMs in the order of priority.

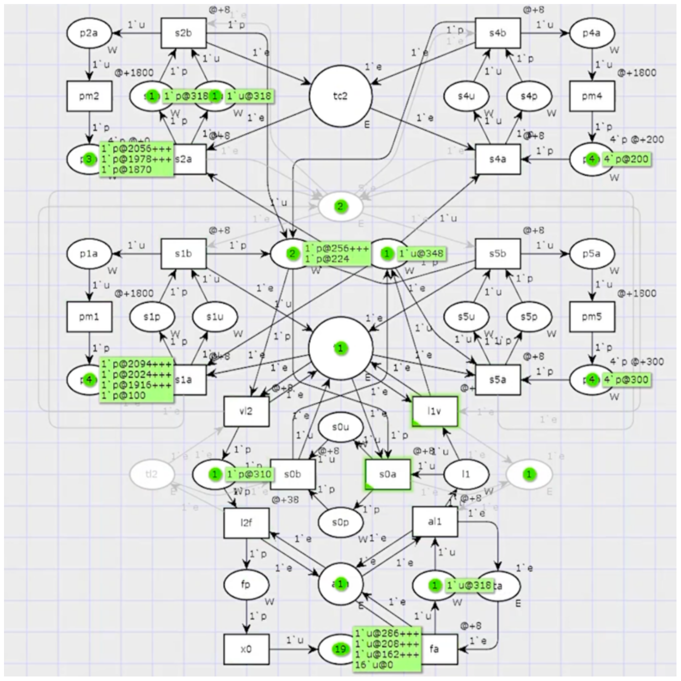
Video 5.4 Clip of video for steady-state simulation of a standard recipe with delayed tokens using CPN Tools available at https://www.youtube.com/watch?v=GHcqyrRj64A.

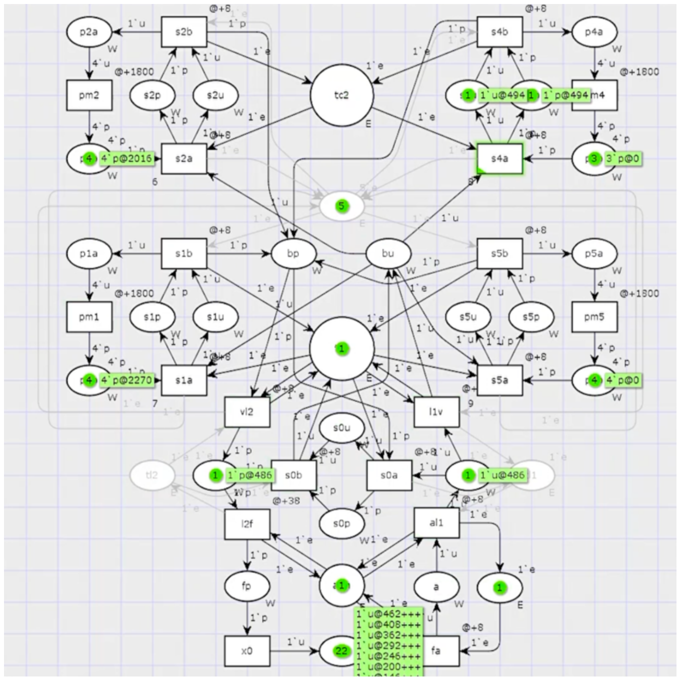
Video 5.5 Clip of video for steady-state simulation of a static recipe with priority transitions using CPN Tools available at https://www.youtube.com/watch?v=DSTGq8cbDKw.

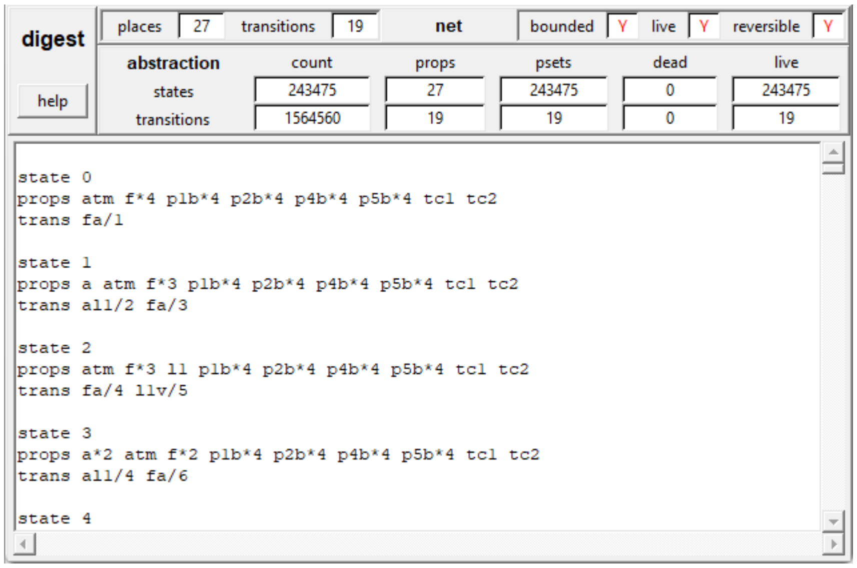

places	27	transitions	19	bounded	Y	live	Y	reversible	Y

	count	props	psets	dead	live
states	243475	27	243475	0	243475
transitions	1564560	19	19	0	19

```
state 0
props atm f*4 p1b*4 p2b*4 p4b*4 p5b*4 tc1 tc2
trans fa/1

state 1
props a atm f*3 p1b*4 p2b*4 p4b*4 p5b*4 tc1 tc2
trans a11/2 fa/3

state 2
props atm f*3 l1 p1b*4 p2b*4 p4b*4 p5b*4 tc1 tc2
trans fa/4 l1v/5

state 3
props a*2 atm f*2 p1b*4 p2b*4 p4b*4 p5b*4 tc1 tc2
trans a11/4 fa/6

state 4
```

Figure 5.4 Analysis of steady-state Petri net in TINA.

As shown in Figure 5.4, the steady-state Petri net is bounded, live and reversible. TINA also generated the reachability states, as shown. There are 243,475 states in total, with 1,564,560 transitions generated from 27 places with 19 transitions. One thing to note here is that the states are being minimized with the use of only four wafers in the FOUP. By increasing the number of wafers in the FOUP, the number of states and transitions will increase while maintaining its properties of boundedness, liveness, and reversibility.

5.3 Initial Transient Process

The initial transient process brings the system to meet steady-state conditions. All the PMs prior to the initial transient process are empty. Depending on how many wafers are to be loaded, there are four different cases to consider having an optimal start. Even though the cluster tool has a dual robot arm, for this process, it will behave as though it is operating with a single arm. The objective of the initial transient process is the minimize the time taken to fill the pipeline of wafers into the system to either achieve the steady-state or initiate the final transient process, depending on the number of wafers that need to be processed. There is a specific strategy to deploy, as there are two distinct durations to get the wafers to different PMs.

The first type of operation for loading wafers is the one involving PM_1 and PM_5, in which the wafer is:

1. unloaded from the FOUP and loaded into the aligner by the atmosphere robot ($\omega_{ia} + 2\mu + \omega_{if}$)
2. unloaded from the aligner, after alignment, and loaded into the inbound loadlock by the atmosphere robot ($\rho + \omega_{ia} + 2\mu + \omega_{il}$)
3. unloaded from the inbound loadlock and loaded into PM_1 or PM_5 by the transfer chamber 1 robot ($\lambda + \omega_{il} + 2\mu + \omega_{ip}$)

The second type of operation for loading wafers is the one involving PM_2 and PM_4, in which the wafer is:

1. unloaded from the FOUP and loaded into the aligner by the atmosphere robot ($\omega_{ia} + 2\mu + \omega_{if}$)
2. unloaded from the aligner, after alignment, and loaded into the inbound loadlock by the atmosphere robot ($\rho + \omega_{ia} + 2\mu + \omega_{il}$)
3. unloaded from the inbound loadlock and loaded into the vacuum buffer by the transfer chamber 1 robot ($\lambda + \omega_{il} + 2\mu + \omega_{iv}$)
4. unloaded from the vacuum buffer and loaded into the PM_2 or PM_4 by the transfer chamber 2 robot ($\omega_{iv} + 2\mu + \omega_{ip}$)

Ceteris paribus, with other conditions remaining the same, the second type of operation takes 2μ longer, as $\omega_{iv} = 0$, than the first and holds the key to the strategy on how to place wafers when minimizing the initial transient process. Since we are working with quad station modules, depending on the number of wafers involved, the process has repetitions, yet it is not cyclic as it is in a steady-state.

Let the number of wafers to be processed be w.

Case 1 ($w \leq 8$): The wafers can be loaded into either PM$_1$ and/or PM$_5$, with a priority for filling a single PM first. In this case, the system will not enter the steady-state and proceed to the final transient process after this.

Case 2 ($8 < w \leq 12$): The key here is the 2μ time difference between the two types of operations. To do so efficiently, we need to schedule the first type of operation (meaning use either PM$_1$ or PM$_5$) first, followed by the second type of operation (meaning use either PM$_2$ or PM$_4$). Then alternate back to the first type of operation with the use of either PM$_1$ or PM$_5$. The system will not enter the steady-state in this case either and execute the final transient process.

Case 3 ($12 < w < 16$): For this case, there needs to be at least a single alternating event between the two different operations when scheduling the first 2 PMs. Some examples: PM$_1$ → PM$_2$ → PM$_4$ → PM$_5$ or PM$_2$ → PM$_1$ → PM$_4$ → PM$_5$.This will take advantage of the 2μ time difference. The system will not enter the steady-state in this case either and execute the final transient process afterward.

Case 4 ($w \geq 16$): In this case, all the PMs would be filled. However, as in case 3, we need to alternate between the two operations when scheduling the first 2 PMs. The system will then meet the conditions of the steady-state when all the PMs are filled. It will then be followed by the final transient process when the new wafers run out.

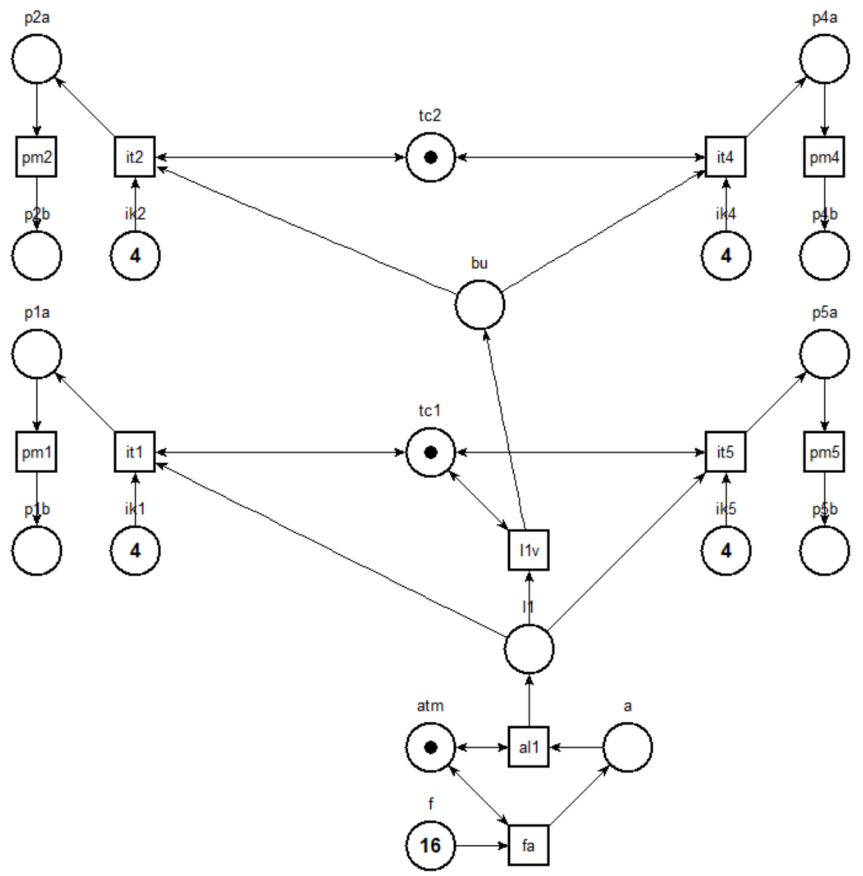

Figure 5.5 Initial transient process Petri net.

The Petri net being used is a separate and modified version of the standard recipe Petri net. It keeps the wafer input elements. At each PM, we have an additional transition (it_i) and an additional place (ik_i), $K(ik_i) = 4$ and $i \in \mathbb{N}_n$, where $\mathbb{N}_n = \{1,2,4,5\}$. The transition models the transfer operation of wafers to the PM, and the place models the finite capacity control of a quad station module. We can think of this as a sub-system with distinct and compartmentalized behavior for filling the pipeline, mostly to achieve the steady-state, at which point, the steady-state Petri net will be used.

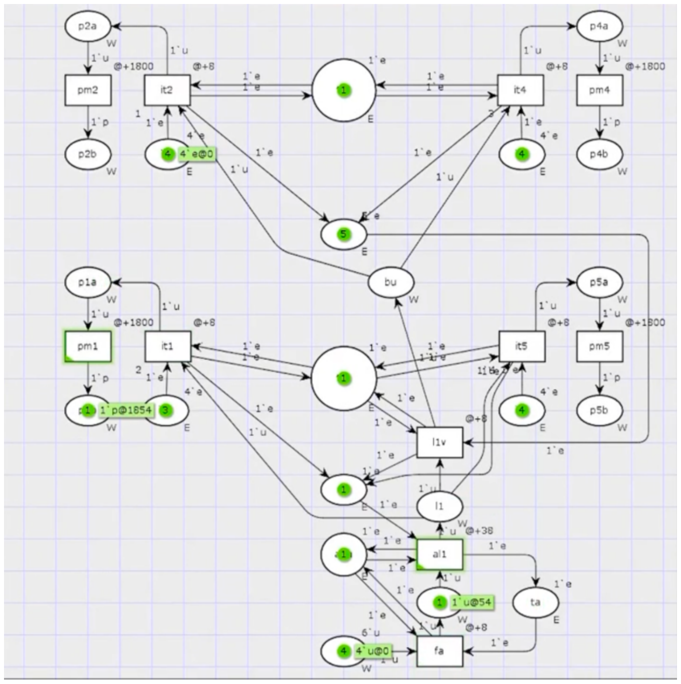
Video 5.6 Clip of video for initial transient process with a different number of wafers and cases simulation using CPN Tools available at https://www.youtube.com/watch?v=jQFtO3G_wu4.

As shown in Figure 5.6, the initial transient process Petri net is bounded but not live nor reversible. It is not expected to be either live or reversible as the task is to fill the system with wafers, and it has a specific end condition at which the net will be switched over to a steady-state or final transient process. TINA also generated the reachability states, as shown. There are 4,459,125 states in total, with 30,034,000 transitions generated from 19 places with 11 transitions. Although it is a simpler net relative to the steady-state, it does have significantly more states in comparison to the steady-state due to the use of more wafers in the FOUP for the analysis.

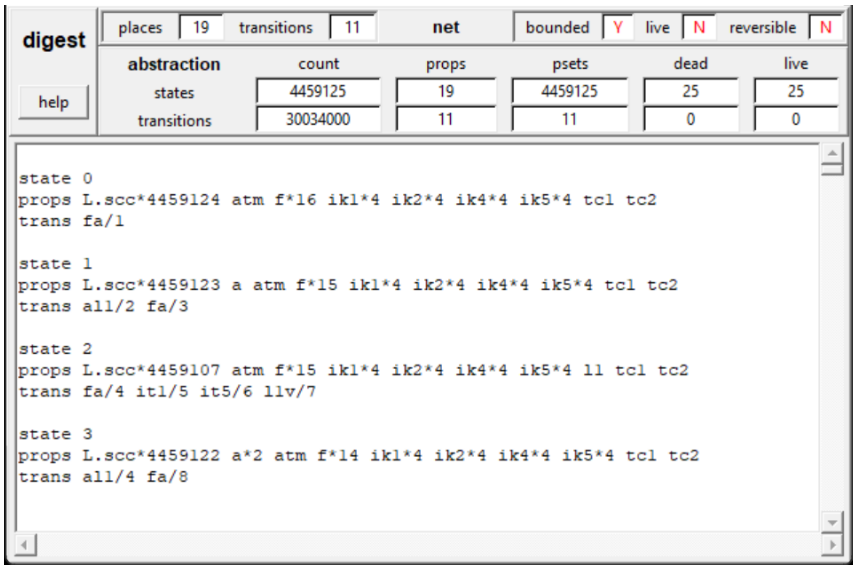

abstraction	count	props	psets	dead	live
states	4459125	19	4459125	25	25
transitions	30034000	11	11	0	0

```
state 0
props L.scc*4459124 atm f*16 ik1*4 ik2*4 ik4*4 ik5*4 tc1 tc2
trans fa/1

state 1
props L.scc*4459123 a atm f*15 ik1*4 ik2*4 ik4*4 ik5*4 tc1 tc2
trans al1/2 fa/3

state 2
props L.scc*4459107 atm f*15 ik1*4 ik2*4 ik4*4 ik5*4 l1 tc1 tc2
trans fa/4 it1/5 it5/6 l1v/7

state 3
props L.scc*4459122 a*2 atm f*14 ik1*4 ik2*4 ik4*4 ik5*4 tc1 tc2
trans al1/4 fa/8
```

Figure 5.6 Analysis of initial transient process Petri net in TINA.

5.4 Final Transient Process

The final transient process winds down the system from the steady-state. The process needs to meet the following condition: $M(f) = M(a) = M(l_1) = M(b_u) = 0$ What this means is that there are no more new wafers in either the FOUP, aligner, inbound loadlock, or buffer. Once this condition is met, for the system, based on the availability of the processed wafers, the wafers would be removed. As we can see in Video 5.7, as the processed wafers become available, each is removed from the system. (In the simulation, there are additional places (ft_{ip} and tft_i) and transitions (ft_{it}) to simulate the staggering availability of wafers that will be produced by the steady-state.)

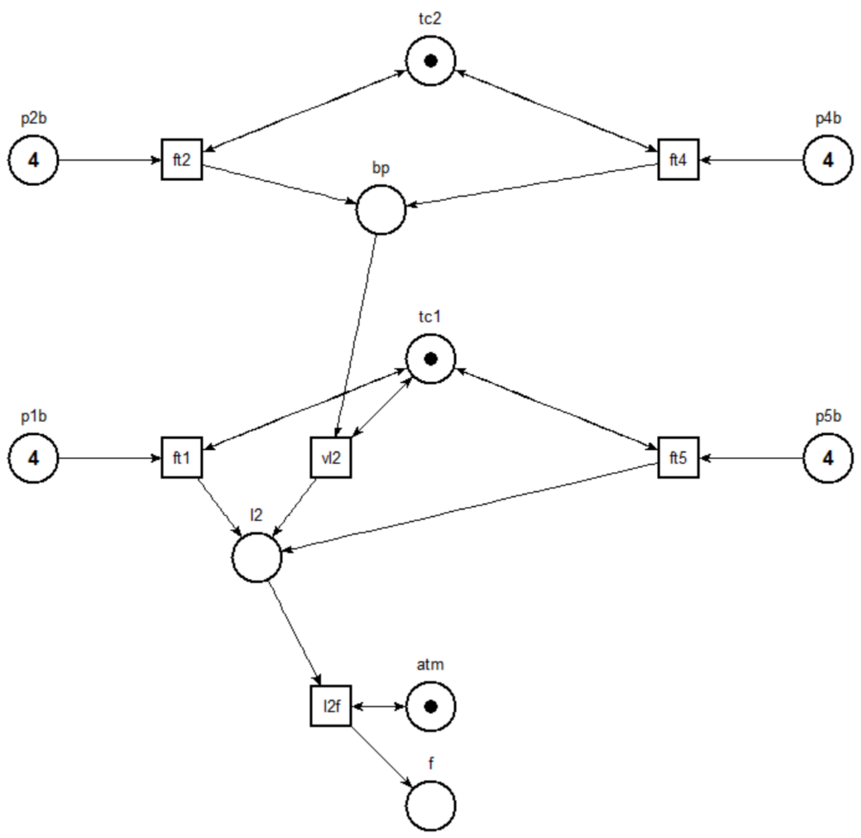

Figure 5.7 Final transient process Petri net.

As shown in Figure 5.8, the final transient process Petri net is bounded but not live nor reversible. It is also a simpler system relative to the steady-state and the initial transient process. TINA also generated the reachability states, as shown. There are 23,125 states in total, with 104,000 transitions generated from 10 places and 6 transitions.

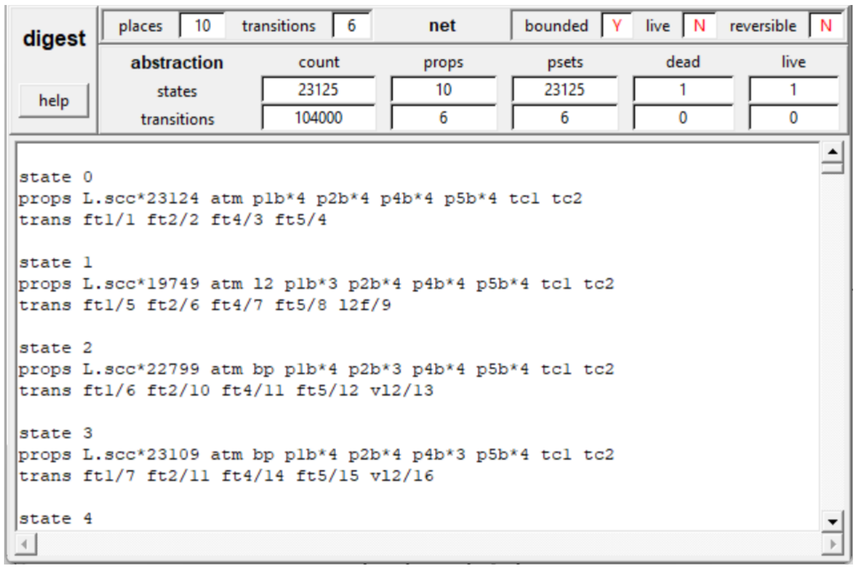

digest | places 10 | transitions 6 | net | bounded Y | live N | reversible N

help

abstraction	count	props	psets	dead	live
states	23125	10	23125	1	1
transitions	104000	6	6	0	0

```
state 0
props L.scc*23124 atm p1b*4 p2b*4 p4b*4 p5b*4 tc1 tc2
trans ft1/1 ft2/2 ft4/3 ft5/4

state 1
props L.scc*19749 atm l2 p1b*3 p2b*4 p4b*4 p5b*4 tc1 tc2
trans ft1/5 ft2/6 ft4/7 ft5/8 l2f/9

state 2
props L.scc*22799 atm bp p1b*4 p2b*3 p4b*4 p5b*4 tc1 tc2
trans ft1/6 ft2/10 ft4/11 ft5/12 vl2/13

state 3
props L.scc*23109 atm bp p1b*4 p2b*4 p4b*3 p5b*4 tc1 tc2
trans ft1/7 ft2/11 ft4/14 ft5/15 vl2/16

state 4
```

Figure 5.8 Analysis of final transient process Petri net in TINA.

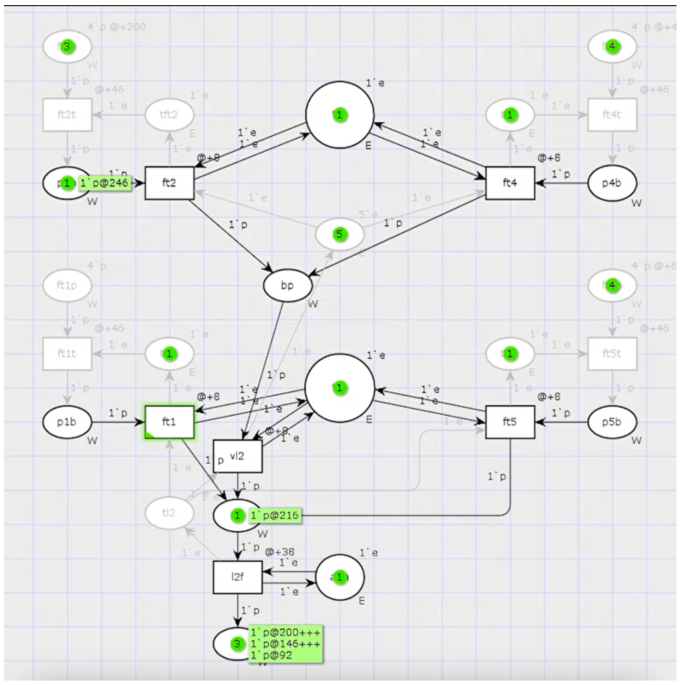

Video 5.7 Clip of video for final transient process simulation using CPN Tools available at https://www.youtube.com/watch?v=xnXOXkpKfcg.

CHAPTER 6

CONCLUSION

The scheduling component of a semiconductor cluster tool is an expansive endeavor that requires highly experienced developers and engineers and a task that is growing in complexity every day. It is also the least researched area in the semiconductor industry. [4] As such, there could be undiscovered optimizations and improvements that might exist that have not been researched. Petri nets are one of the areas that could use more investment.

So far, Petri net scheduling of the cluster tool works well as long as the configuration of the cluster tool is static. However, that is not the reality of the semiconductor industry. The configurations of cluster tools are constantly changing with the desire for different behavior. That would require constant redevelopment of a new Petri net model, which is not trivial, without the ability to fully leverage the existing models. As the Petri net model increases in size, the computational complexity also increases exponentially, which is not tenable in the long term as the complexity of the cluster tools increases.

Modeling production cluster tools with real-world non-elegant requirements take away the elegance of existing theoretical solutions. Another area that requires exploration is the efficacy of switching between Petri net models for scheduling a heuristic rule-based approach. The relative computational and development cost should be researched.

On the other hand, Petri net models can be a great tool to deploy along with the heuristic rule-based approach at the launch of a new tool or configuration, as the model can explore the states that might or might not be encountered by developers as part of the testing and trial-and-error process. The Petri net model can catch the deadlocks, and other undesirable states, mathematically. A Petri net model can be a foundation from which the developers' experience and creativity can evolve from, shortening the development time and allowing for the delivery of a more mature ruleset to market at launch.

APPENDIX A

GRAPHS & PROGRAM

Based on Dr. Zhao's insight into Petri net's ability to see over the horizon to make decisions on scheduling, the reachability graph was explored to calculate strongly connected components using Tarjan's algorithm, nodes of n-walks, and the shortest path using Dijkstra's algorithm. Google Colab for Python notebook was used, and the Network-X package was leveraged. The work is shared at: https://drive.google.com/drive/folders/18KzRtacbeJT1OnDbhKEW1Mq54SHGN6Lj.

The motivation of the Python notebook is an exercise to take the output files from TINA and create multi-directed graphs, which we can use to get strongly connected components, shortest paths between states, and states of n-walk. We also wanted to filter the results using the number of tokens at different places to identify good or bad states. In general, any code cell is dependent on the prior code cells. Each code cell can be run independently, assuming all dependent cells have been run before.

The notebook has nine sections:

1. Overview
2. Libraries
3. File Import
4. Parsing Input
5. Make Graph
6. States Filter
7. Strongly Connected Components
8. N-Walks from a Node

9. Shortest Path(s)

The input file is imported as a dataframe from Google Drive by mounting Google Drive. If running this notebook locally, please comment out the Google Drive mount code and change that path to the appropriate input file that you would like to use. The input file is the output of the TINA Marking Graph (option-R). (Note: Please make sure to scroll all the way to the end of the TINA output prior to saving to ensure the full text is saved from TINA.)

For parsing, the input text file that is generated has three lines for each state; the first line gives us the state index. The second line gives us the different tokens for each marking/state. If the marking place has no tokens, it is not listed. If it has a single token, the name of the place is listed. If it has more than one token, the place name has a suffix *, which is followed by an integer. The third line gives us the transitions. Each available transition has the transition with a suffix "/", followed by the target state.

This section has five parts:

i. parse_props function: this function takes a list in and returns a dictionary
ii. parse_file function: this function parses the input file and returns a tuple of node_list (tuple of nodes and labels), place_dict (dictionary for markings with places and tokens), and dead_list (list of dead states).
iii. formatting node_list for a more human-readable format. The code is commented out, and its use is optional.
iv. dict_to_dffunction: converts the dictionary to a dataframe, then replaces the NaNs with 0s and typecasts it into int

v. this part prints out the dead state list. The code is commented out, and its use is optional. Only applicable when there are dead states in the input file.

NetworkX library is used to make a multi-directed graph, G, of the reachability graph using the node_list from the previous section (parse_file function). There are three optional code cells:

i. prints the number of nodes and edges
ii. draws the graph (Due to the size of the graph, it is not very usable.)
iii. exports the graph into a .gexf format which can be read by the Gephi application to draw graphs.

States Filter is an optional section that takes the props_df generated by diet_to_df from the parsing input section and filters using the number of tokens in places. The first two code cells give us basic information about the dataframe to edit the filter.

For Strongly Connected Components, the program takes the multi-directed graph, G, from the NetworkX section and gets basic information about the G graph in terms of SCCs: how many there are, the length of each, and the largest SCC in the G graph using Tarjan's algorithm.

Based on the information gathered above, the n-walk function can be used to get the dataframe of nodes and their associated state information of states that are a certain distance from the source node, given a graph.

Based on the information gathered above, get the list of all available shortest paths, using Dijkstra's algorithm, from a source state to a target state.

Memory usage was measured with both psutil and tracemalloc. psutil measures the memory usage by the Python interpreter, and tracemalloc measures the Python dynamic memory allocation on the heap.

In Figure A.1, we can see both psutil and tracemalloc outputs for each function. For each function, we have a psutil that gives us the line-by-line memory usage with increments and occurrences. This is followed by current and peak memory usage by tracemalloc. For example, the function run_nx, which uses NetworkX to add edges and their corresponding labels, has incremental memory usage of (43.3 + 774.7 MiB) as per psutil, while tracemalloc shows that the function uses 648.25 MiB at peak.

The get_sec function, which gets the number of strongly connected components (SCC), their length(s), and printing the largest SCC, use 63.23 MiB at peak, according to tracemalloc, with only 0.6 MiB use according to psutil. The n-walk and shortest path functions also use 63.23 and 0.03 MiB, respectively, at peak.

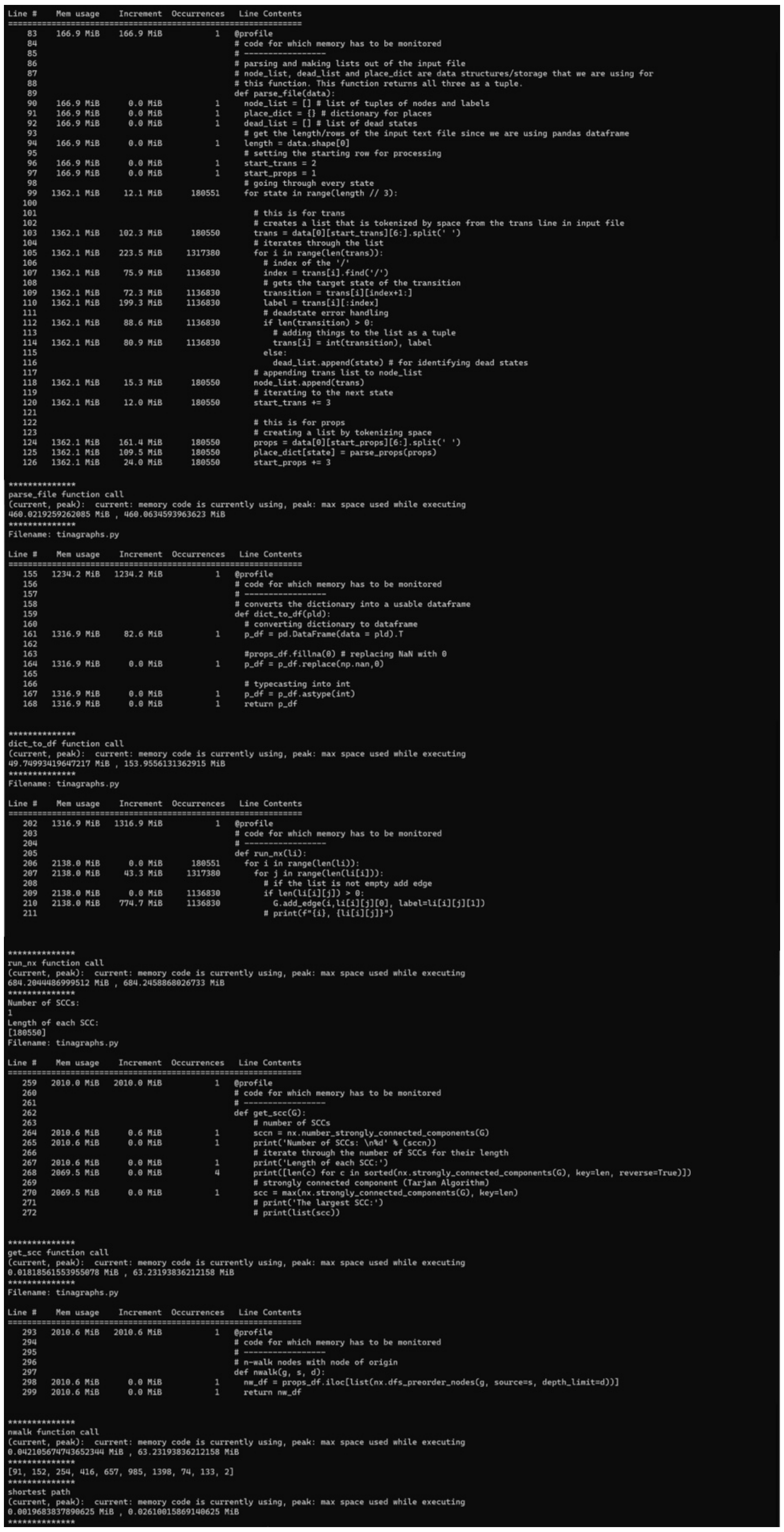

```
Line #    Mem usage    Increment  Occurrences   Line Contents
=============================================================
    83    166.9 MiB    166.9 MiB           1   @profile
    84                                         # code for which memory has to be monitored
    85                                         # -----------------
    86                                         # parsing and making lists out of the input file
    87                                         # node_list, dead_list and place_dict are data structures/storage that we are using for
    88                                         # this function. This function returns all three as a tuple.
    89                                         def parse_file(data):
    90    166.9 MiB      0.0 MiB           1     node_list = [] # list of tuples of nodes and labels
    91    166.9 MiB      0.0 MiB           1     place_dict = {} # dictionary for places
    92    166.9 MiB      0.0 MiB           1     dead_list = [] # list of dead states
    93                                           # get the length/rows of the input text file since we are using pandas dataframe
    94    166.9 MiB      0.0 MiB           1     length = data.shape[0]
    95                                           # setting the starting row for processing
    96    166.9 MiB      0.0 MiB           1     start_trans = 2
    97    166.9 MiB      0.0 MiB           1     start_props = 1
    98                                           # going through every state
    99   1362.1 MiB     12.1 MiB      180551     for state in range(length // 3):
   100
   101                                             # this is for trans
   102                                             # creates a list that is tokenized by space from the trans line in input file
   103   1362.1 MiB    102.3 MiB      180550       trans = data[0][start_trans][6:].split(' ')
   104                                             # iterates through the list
   105   1362.1 MiB    223.5 MiB     1317380       for i in range(len(trans)):
   106                                               # index of the '/'
   107   1362.1 MiB     75.9 MiB     1136830         index = trans[i].find('/')
   108                                               # gets the target state of the transition
   109   1362.1 MiB     72.3 MiB     1136830         transition = trans[i][index+1:]
   110   1362.1 MiB    199.3 MiB     1136830         label = trans[i][:index]
   111                                               # deadstate error handling
   112   1362.1 MiB     88.6 MiB     1136830         if len(transition) > 0:
   113                                                 # adding things to the list as a tuple
   114   1362.1 MiB     80.9 MiB     1136830           trans[i] = int(transition), label
   115                                               else:
   116                                                 dead_list.append(state) # for identifying dead states
   117                                             # appending trans list to node_list
   118   1362.1 MiB     15.3 MiB      180550       node_list.append(trans)
   119                                             # iterating to the next state
   120   1362.1 MiB     12.0 MiB      180550       start_trans += 3
   121
   122                                             # this is for props
   123                                             # creating a list by tokenizing space
   124   1362.1 MiB    161.4 MiB      180550       props = data[0][start_props][6:].split(' ')
   125   1362.1 MiB    109.5 MiB      180550       place_dict[state] = parse_props(props)
   126   1362.1 MiB     24.0 MiB      180550       start_props += 3

**************
parse_file function call
(current, peak):  current: memory code is currently using, peak: max space used while executing
460.0219259262085 MiB , 460.0634593963623 MiB
**************
Filename: tinagraphs.py

Line #    Mem usage    Increment  Occurrences   Line Contents
=============================================================
   155   1234.2 MiB   1234.2 MiB           1   @profile
   156                                         # code for which memory has to be monitored
   157                                         # -----------------
   158                                         # converts the dictionary into a usable dataframe
   159                                         def dict_to_df(pld):
   160                                           # converting dictionary to dataframe
   161   1316.9 MiB     82.6 MiB           1     p_df = pd.DataFrame(data = pld).T
   162
   163                                           #props_df.fillna(0) # replacing NaN with 0
   164   1316.9 MiB      0.0 MiB           1     p_df = p_df.replace(np.nan,0)
   165
   166                                           # typecasting into int
   167   1316.9 MiB      0.0 MiB           1     p_df = p_df.astype(int)
   168   1316.9 MiB      0.0 MiB           1     return p_df


**************
dict_to_df function call
(current, peak):  current: memory code is currently using, peak: max space used while executing
49.74993419647217 MiB , 153.9556131362915 MiB
**************
Filename: tinagraphs.py

Line #    Mem usage    Increment  Occurrences   Line Contents
=============================================================
   202   1316.9 MiB   1316.9 MiB           1   @profile
   203                                         # code for which memory has to be monitored
   204                                         # -----------------
   205                                         def run_nx(li):
   206   2138.0 MiB      0.0 MiB      180551     for i in range(len(li)):
   207   2138.0 MiB     43.3 MiB     1317380       for j in range(len(li[i])):
   208                                               # if the list is not empty add edge
   209   2138.0 MiB      0.0 MiB     1136830         if len(li[i][j]) > 0:
   210   2138.0 MiB    774.7 MiB     1136830           G.add_edge(i,li[i][j][0], label=li[i][j][1])
   211                                               # print(f"{i}, {li[i][j]}")


**************
run_nx function call
(current, peak):  current: memory code is currently using, peak: max space used while executing
684.2044486999512 MiB , 684.2458868026733 MiB
**************
Number of SCCs:
1
Length of each SCC:
[180550]
Filename: tinagraphs.py

Line #    Mem usage    Increment  Occurrences   Line Contents
=============================================================
   259   2010.0 MiB   2010.0 MiB           1   @profile
   260                                         # code for which memory has to be monitored
   261                                         # -----------------
   262                                         def get_scc(G):
   263                                             # number of SCCs
   264   2010.6 MiB      0.6 MiB           1       sccn = nx.number_strongly_connected_components(G)
   265   2010.6 MiB      0.0 MiB           1       print('Number of SCCs: \n%d' % (sccn))
   266                                             # iterate through the number of SCCs for their length
   267   2010.6 MiB      0.0 MiB           1       print('Length of each SCC:')
   268   2069.5 MiB      0.0 MiB           4       print([len(c) for c in sorted(nx.strongly_connected_components(G), key=len, reverse=True)])
   269                                             # strongly connected component (Tarjan Algorithm)
   270   2069.5 MiB      0.0 MiB           1       scc = max(nx.strongly_connected_components(G), key=len)
   271                                             # print('The largest SCC:')
   272                                             # print(list(scc))


**************
get_scc function call
(current, peak):  current: memory code is currently using, peak: max space used while executing
0.01818561553955078 MiB , 63.23193836212158 MiB
**************
Filename: tinagraphs.py

Line #    Mem usage    Increment  Occurrences   Line Contents
=============================================================
   293   2010.6 MiB   2010.6 MiB           1   @profile
   294                                         # code for which memory has to be monitored
   295                                         # -----------------
   296                                         # n-walk nodes with node of origin
   297                                         def nwalk(g, s, d):
   298   2010.6 MiB      0.0 MiB           1     nw_df = props_df.iloc[list(nx.dfs_preorder_nodes(g, source=s, depth_limit=d))]
   299   2010.6 MiB      0.0 MiB           1     return nw_df


**************
nwalk function call
(current, peak):  current: memory code is currently using, peak: max space used while executing
0.04210567474365234 MiB , 63.23193836212158 MiB
**************
[91, 152, 254, 416, 657, 985, 1398, 74, 133, 2]
**************
shortest path
(current, peak):  current: memory code is currently using, peak: max space used while executing
0.0019683837890625 MiB , 0.02610015869140625 MiB
**************
```

Figure A.1 Petri net graph memory usage

APPENDIX B

TINA INSTRUCTION

Link to TINA manual https://projects.laas.fr/tina/manuals/tina.html

During my work, the most used function in TINA is building the reachability graph (marking graph). This can be found at Tools> State Space Analysis> -R (with the liveness analysis option checked). If we set the output to default kts (.ktz), it generates a text file in a new window. It lists the number of places and transitions. Then it gives us the analysis of boundedness, liveness, and reversibility. This is then followed by the states and transitions information. First is the count of states and transitions. This is then followed by props, which are the elements of the states and transitions. It is then followed by psets, which is the flow information. Then we get the number of live and dead states and transitions. The text file that is generated has three lines for each state. The first line gives us the state index. The second line gives us the different tokens for each marking/state. If the marking place has no tokens, it is not listed. If it has a single token, the name of the place is listed. If it has more than one token, the place name has a suffix '*', which is followed by an integer. The third line gives us the transitions. Each available transition has the transition with a suffix'/', followed by the index of the target state.

Note: We can save the file as a text file. However, to get the full list, we have to scroll all the way to the end of the document prior to saving it. Otherwise, only a partial list will be saved as a .ktz file. However, you can rename the file as .txt during or after saving the file.

APPENDIX C

CPN TOOLS INSTRUCTION

Link to CPN Tools documentation http://cpntools.org/2018/01/16/documentation-2/

For this exploration purpose, CPN Tools was used as a visual simulator of wafer movement. The simulation files are shared at:

https://drive.google.com/drive/folders/18KzRtacbeJT1OnDbhKEW1Mq54SHGN6Lj.

.cpn file that simulates the wafer flow of batch-begin, batch-end, and steady-state. The simulation is not a circular process. It will only process the number of wafers specified in the cu place. To change the number of wafers in cu, you can click on the value to the top right of the cu place, which is usually an integer followed by ''u', and change the integer value to the number of the wafer you would like to simulate. You can also click on the cu place and press tab to cycle through the parameters of it and change the integer value.

To simulate, please drag the word Simulation from the menu on the left-hand side onto the darker blue area of the application on the right. It will open the Simulation menu. Please press the play button to simulate. The play button has a number below it that specify how many steps it will execute. You can change it by right-clicking on the play button to Set Options for the play button. You can use the rest of the control buttons to control the simulation, including simulating one step at a time.

REFERENCES

[1] B. Berthomieu, F. Vernadat, and S. dal Zilio, "TINA toolbox - TIme petri Net Analyzer - by LAAS/CNRS," *TINA Toolbox*. https://projects.laas.fr/tina/index.php (accessed Jul. 12, 2022).

[2] CPN Tools, "Anti places/limit places – CPN Tools," *CPN Tools*, Jan. 11, 2018. https://cpntools.org/2018/01/11/anti-places-limit-places/ (accessed Jun. 11, 2022).

[3] CPN Tools, "CPN Tools – A tool for editing, simulating, and analyzing Colored Petri nets," *CPN Tools*. https://cpntools.org (accessed Dec. 13, 2022).

[4] J. W. Fowler, "Scheduling Problems in Semiconductor Wafer Fabrication Facilities: Part 1," *https://schedulingseminar.com/*, Mar. 03, 2022. https://www.youtube.com/watch?v=5ZCtbU1VR3s (accessed Mar. 04, 2022).

[5] B. Hrúz and M. Zhou, *Modeling and Control of Discrete-event Dynamic Systems*. Springer Science & Business Media, 2007.

[6] O. Kilincci, "A Petri net-based heuristic for simple assembly line balancing problem of type 2," *The International Journal of Advanced Manufacturing Technology*, vol. 46, no. 1–4, pp. 329–338, Jan. 2010, doi: 10.1007/s00170-009-2082-z.

[7] C. A. Petri, "Kommunikation mit Automaten," Dissertation, Universität Hamburg, 1962.

[8] C. Petri and W. Reisig, "Petri net," *Scholarpedia*, vol. 3, no. 4, p. 6477, 2008, doi: 10.4249/scholarpedia.6477.

[9] Y. Qiao, M. Zhou, N. Wu, Z. Li, and Q. Zhu, "Closing-Down Optimization for Single-Arm Cluster Tools Subject to Wafer Residency Time Constraints," *IEEE Transactions on Systems, Man, and Cybernetics: Systems*, vol. 51, no. 11, pp. 6792–6807, Nov. 2021, doi: 10.1109/tsmc.2020.2964032.

[10] J. Wang, H. Hu, C. Pan, Y. Zhou, and L. Li, "Scheduling dual-arm cluster tools with multiple wafer types and residency time constraints," *IEEE/CAA Journal of Automatica Sinica*, vol. 7, no. 3, pp. 776–789, May 2020, doi: 10.1109/jas.2020.1003150.

[11] S. Wang *et al.*, "Computation of an emptiable minimal siphon in a subclass of Petri nets using mixed-integer programming," *IEEE/CAA Journal of Automatica Sinica*, vol. 8, no. 1, pp. 219–226, Jan. 2021, doi: 10.1109/jas.2020.1003210.

[12] Wikipedia Contributors, "Petri net," *Wikipedia*, Nov. 08, 2019. https://en.wikipedia.org/wiki/Petri_net (accessed Nov. 18, 2021).

[13] N. Q. Wu and M. Zhou, "A Closed-Form Solution for Schedulability and Optimal Scheduling of Dual-Arm Cluster Tools With Wafer Residency Time Constraint Based on Steady Schedule Analysis," *IEEE Transactions on Automation Science and Engineering*, vol. 7, no. 2, pp. 303–315, Apr. 2010, doi: 10.1109/tase.2008.2008633.

[14] H. H. Xiong and M. Zhou, "Scheduling of semiconductor test facility via Petri nets and hybrid heuristic search," *IEEE Transactions on Semiconductor Manufacturing*, vol. 11, no. 3, pp. 384–393, Aug. 1998, doi: 10.1109/66.705373.

[15] F. Yang, N. Wu, Y. Qiao, M. Zhou, and Z. Li, "Scheduling of Single-Arm Cluster Tools for an Atomic Layer Deposition Process With Residency Time Constraints," *IEEE Transactions on Systems, Man, and Cybernetics: Systems*, vol. 47, no. 3, pp. 502–516, Mar. 2017, doi: 10.1109/tsmc.2015.2507140.

[16] Z. Zhao, S. Liu, M. Zhou, D. You, and X. Guo, "Heuristic Scheduling of Batch Production Processes Based on Petri Nets and Iterated Greedy Algorithms," *IEEE Transactions on Automation Science and Engineering*, vol. 19, no. 1, pp. 251–261, Jan. 2022, doi: 10.1109/tase.2020.3027532.

[17] M. Zhou and K. Venkatesh, Modeling, Simulation, and Control of Flexible Manufacturing Systems : A Petri Net Approach. Singapore: World Scientific, 1999.

[18] M. Zhou and N. Wu, *System Modeling and Control with Resource-Oriented Petri Nets*. New York: CRC Press, 2017.

[19] Q. Zhu, M. Zhou, Y. Qiao, and N. Wu, "Petri Net Modeling and Scheduling of a Close-Down Process for Time-Constrained Single-Arm Cluster Tools," *IEEE Transactions on Systems, Man, and Cybernetics: Systems*, vol. 48, no. 3, pp. 389–400, Mar. 2018, doi: 10.1109/tsmc.2016.2598303.

[20] Q. Zhu, Y. Qiao, N. Wu, and Y. Hou, "Post-processing time-aware optimal scheduling of single robotic cluster tools," *IEEE/CAA Journal of Automatica Sinica*, vol. 7, no. 2, pp. 597–605, Mar. 2020, doi: 10.1109/jas.2020.1003069.

[21] R. Zurawski and M. Zhou, “Petri Nets and Industrial Applications: A Tutorial,” IEEE Transactions on Industrial Electronics, vol. 41, no. 6, pp. 567–583, 1994, doi: 10.1109/41.334574.